



OPEN ACCESS

EDITED BY

Carlos Gregorio Barreras-Urbina,
National Council of Science and Technology
(CONACYT), Mexico

REVIEWED BY

José Agustín Tapia Hernández,
University of Sonora, Mexico
Yongsheng Chen,
Jinan University, China

*CORRESPONDENCE

Jiangning Zhang
✉ zhangjiangning2022@163.com

RECEIVED 05 February 2024

ACCEPTED 12 April 2024

PUBLISHED 24 April 2024

CITATION

Zhang J and Ye Z (2024) Influences of superfine-grinding and mix enzymatic hydrolysis combined with hydroxypropylation or acetylation on the structure and physicochemical properties of jujube kernel fiber.

Front. Sustain. Food Syst. 8:1382314.
doi: 10.3389/fsufs.2024.1382314

COPYRIGHT

© 2024 Zhang and Ye. This is an open-access article distributed under the terms of the [Creative Commons Attribution License \(CC BY\)](https://creativecommons.org/licenses/by/4.0/). The use, distribution or reproduction in other forums is permitted, provided the original author(s) and the copyright owner(s) are credited and that the original publication in this journal is cited, in accordance with accepted academic practice. No use, distribution or reproduction is permitted which does not comply with these terms.

Influences of superfine-grinding and mix enzymatic hydrolysis combined with hydroxypropylation or acetylation on the structure and physicochemical properties of jujube kernel fiber

Jiangning Zhang* and Zheng Ye

Shanxi Functional Food Research Institute of Shanxi Agricultural University, Taiyuan, China

Introduction: Jujube kernel is a low-cost and abundant fiber resource, but its application in food industry is little because of its lower soluble fiber content and poor physicochemical properties.

Methods: In the current study, jujube kernel fiber (JKF) was modified by three composite methods: superfine-grinding and mix enzymatic hydrolysis alone, and combined with acetylation or hydroxypropylation.

Results and discussion: After these modifications, the microstructure of JKF became more porous, and its soluble fiber and extractable polyphenol contents, surface area, water adsorption and expansion capacities, and cation exchange capacity were all significantly improved ($p < 0.05$). Moreover, superfine-grinding and mix enzymatic hydrolysis combined with acetylation treated JKF showed the highest surface hydrophobicity (43.57) and adsorption ability to oil (4.47 g•g⁻¹). Superfine-grinding, mix enzymatic hydrolysis and hydroxypropylation treated JKF exhibited the largest surface area (142.53 m²•kg⁻¹), the highest soluble fiber content (17.43 g•100 g⁻¹), viscosity (14.54 cP), adsorption capacity to glucose (29.61 μmol•g⁻¹), cation exchange capacity (40.82), and water expansion ability (7.60 mL•g⁻¹). Therefore, superfine-grinding and mix enzymatic hydrolysis combined with hydroxypropylation or acetylation were both good choice to improve the physicochemical properties of JKF.

KEYWORDS

jujube kernel fiber, superfine-grinding, mix enzymatic hydrolysis, hydroxypropylation, acetylation, physicochemical properties

1 Introduction

The important role of dietary fiber (DF) in the balance of sugar and fat metabolism has been widely reported, and DF can greatly reduce the incidence of constipation, hyperlipidemia, diabetes, colon cancer and other diseases (Qin et al., 2023). In addition, different industrial food processes generate fiber as a byproduct, for example, the starch industry and the ethanol and bioethanol industry generate a large amount of fiber that can be used to reduce the prevalence of the above diseases (Tapia-Hernández et al., 2019a).

DF is one main component of slimming products such as slimming tea. Moreover, DF can be applied as ingredients of emulsifier, antioxidant, thickener and absorbent to improve the texture, color, flavor, and shelf-life of food (Elleuch et al., 2011). The daily recommended amount of dietary fiber by FAO/WHO is 25–35 g/d, of which the content of soluble dietary fiber (SDF) is not less than 30% (Siddiqui et al., 2023). Plant fiber is the main source of DF, but the content of SDF in most plant fibers, especially grain, vegetable, oil seed and nut fibers, is generally less than 10% (Torbica et al., 2022). Although insoluble dietary fiber (IDF) is also critical to the physicochemical and functional properties of DF, increasing studies have evidenced that the hypoglycemic and hypolipidemic properties of DF can be significantly improved as its SDF content or hydrophilicity increased (Zheng et al., 2022). SDF can increase the viscosity of digestive fluid, or inhibit the activity of major glycoenzymes and lipases in the gastrointestinal tract, thereby delaying the digestion and absorption of sugars and lipids (Hua et al., 2019). In recent years, increasing studies have demonstrated that physical modification (e.g., ultrasound, grafting, heating and high-pressure), biological modification (like cellulase, hemicellulase and Laccase hydrolysis, and fermentation), or chemical modification (such as hydroxypropylation, carboxymethylation, acetylation, and grafting) can improve the hydrophobicity, SDF content, and functional properties of DFs (Gil-López et al., 2019; Zhu et al., 2022; Ji et al., 2024). Of them, superfine-grinding and enzymatic hydrolysis both can improve functional properties of DFs via cracking their glucosidic bonds and releasing groups of high hydrophilicity including free hydroxyl, carboxyl, phenolic and uronic acid groups; while hydroxypropylation and acetylation can enhance the hydrophilicity and hydrophobicity of DFs by grafting hydroxypropyl and acetyl groups into the polysaccharide chains of DFs, respectively (Backes et al., 2021; Zheng et al., 2023). However, to our best knowledge, the synergistic effects of physical, biological and chemical modifications on fibers are rarely studied.

Jujube (*Ziziphus jujuba* Mill.) is one of the main fruit in north of China with a cultivated history of around 4,000 years (Cai et al., 2020). Jujube kernel, a potential dietary fiber resource, is rich in fiber, of which cellulose and lignin account for around 49 and 24 g•100 g⁻¹, respectively (Agrawal et al., 2023). Every year, approximately 200,000 tons of jujube kernels are produced in China, but most of them are discarded directly, and only a small part is used as medicine for nourishing the liver, calming the heart and calming the mind (Bai et al., 2016). Although jujube kernel fiber (JKF) has relatively high water sorption ability, its SDF content (6.32 g•100 g⁻¹) is low and its hypoglycemic and hypolipidemic properties are poor (Ji et al., 2020; Rashwan et al., 2020). Moreover, alkaline treatment has been shown to be effective in reducing cellulose content of date-pits fibers (Al-Khalili et al., 2021), but data referring to modifications of JKF, especially the synergistic effects of physical, chemical and biological modifications on its functional properties is little. Thus, to improve the functional properties of JKF, superfine-grinding and enzymolysis (cellulase and Laccase hydrolysis), superfine-grinding and enzymolysis assisted with acetylation or hydroxypropylation were used to modify JKF. Changes in the structure and physicochemical properties by these composite modification methods were investigated with the purpose of expanding the usage of JKF in food industry.

2 Materials and methods

2.1 Materials

Jujube kernels were purchased from Zaohua Red Jujube Processing Factory, Taigu, China. Laccase (75 U•g⁻¹, one unit corresponds to the amount of enzymes which converts 1 μmol catechol per hour at pH 5.0 and 25°C), hemicellulase (from *Aspergillus Niger*, 2.0 × 10⁵ U•g⁻¹, one unit will liberate 1.0 μmol of D-galactose from hemicellulose per hour at pH 5.5 at 37°C), cellulase (from *Trichoderma Vride G*, 3.0 × 10⁵ U•g⁻¹, one unit corresponds to the amount of enzymes which converts 1 μmol substrate to produce glucose per hour at pH 4.8 and 50°C), amyloglucosidase (*Aspergillus niger*, 1.0 × 10⁵ U•g⁻¹, one unit corresponds to the amount of enzymes which converts 1 μmol soluble starch per minute at pH 4.6 and 40°C), and α-amylase (*Bacillus licheniformis*, 1.0 × 10⁵ U•g⁻¹, one unit corresponds to the amount of enzymes which converts 1 μmol starch to produce glucose per hour at pH 6.9 and 25°C) were all purchased from Peisun Enzyme Company (Nanning, China). The β-D-glucan from oat was purchased from Shanghai Yuanye Biotechnology Co., LTD (Shanghai, China). Monochloroacetic acid, isopropenyl acrylate and other analytical reagents were from Maoyuan Chemical Reagent Company (Tianjin, China).

2.2 JKF preparation

Jujube seed was dried at 45°C for 12 h, and then grinded and sieved with a XL-30C grinder (Xulang Machinery, Guangzhou, China) and a sieve (aperture: 150 μm) (Yushang Sieve Instrument, Shaoxing, China) in sequence. Eighty grams the ground powder, phosphate buffer (100 μmol•L⁻¹, 1 L) and α-amylase (2.4 g) were added and mixed in a triangular glass bottle. The mixture in the bottle was shaken in an HEZ-004C oscillator (Shangxu Instrument Factory, Shangyu, China) at 225 r•min⁻¹ and 90°C, and the pH value of the mixture was maintained at 5.0 through adjusting with NaOH (0.1 mol•L⁻¹) or HCl (0.1 mol•L⁻¹) every 30 min. Ninety minutes later, the mixture was adjusted to pH 7.0 and Papain (1.2 g) was added. The mixture in the bottle was continuously shaken at 225 r•min⁻¹ with the HEZ-004C shaker (50°C, 120 min). Afterward the pH value of the mixture was lowered to 4.0, and then glucoamylase (1.2 g) was added. The bottle was shaken at 225 r•min⁻¹ with the HEZ-004C shaker (60°C, 120 min), and then heated in boiling water for 10 min. Finally, the reaction mixture was filtered by Whatman 1004-047 paper, and the filter residuum on the paper was dried in a GHZ-43B blast drying oven (45°C, 6 h), and JKF was obtained.

2.3 Superfine-grinding and enzymolysis of JKF

The superfine-grinding of JKF was conducted in a JXICSPRP-24L grinder system (Jinxing Grinding Factory, Hangzhou, China). The frequency was 50 Hz and the grinding pressure was 65 MPa (Liu et al., 2021). A laser diffraction analyser (BTE-2200, Betterzer Co., Wuhan, China) was employed to determine the particle size distribution of superfine grinded JKF with an obscuration score of more than 70%.

Next, in a conical flask shaken in the EZH-004C shaker (52°C and 225 r•min⁻¹), JKF dispersed in 0.1 mol•L⁻¹ of phosphate buffer (0.5 g•mL⁻¹, pH 4.5) was hydrolyzed by cellulase (75 U•g⁻¹ JSF) for 2 h (Ma and Mu, 2016). Sodium hydroxide solution (0.2 mol•L⁻¹) was used for adjusting the pH value of the suspension to 6.5±0.1 and the reaction temperature was adjusted to 35.0°C, and then Laccase (25 U•g⁻¹ JKF) was added. The reaction suspension was shaken at 225 r•min⁻¹ for 2 h, and then heated in boiling water for 10 min. Afterward, the suspension was filtered with Whatman1004-047 paper, and the filter residuum on the paper was dried in the GHZ-43B blast drying oven (50°C, 6 h) and superfine-grinding and enzymatic hydrolyzed jujube kernel fiber (JKF-SGE) was obtained.

2.4 Hydroxypropylation of JKF-SGE

JKF-SGE dispersion (0.5 g•mL⁻¹) was pre-incubated at 25°C using the EZH-004C shaker (225 r•min⁻¹, 5 min). Then the pH value of the dispersion was increased to 11.0, and Na₂SO₄ was slowly added until the final concentration was 20 mg•mL⁻¹ (Zheng et al., 2022). Next, propylene oxide (3 mL) was added and the dispersion was shaken at 40°C with the EZH-004C shaker (225 r•min⁻¹). Twenty-four hours later, the reaction dispersion was filtered. The filter residuum was dehydrated with the GHZ-43B dryer (50°C) for 6 h, and then JKF-SGE modified by hydroxypropylation (JKF-SGEH) was collected. The hydroxypropyl degree was measured referring the method of Shaikh et al. (2019).

2.5 Acetylation of JKF-SGE

Twenty grams JSF-SGE were placed in a triangular flask, and dimethyl sulfoxide (270 mL) was slowly added along the inside of the flask (Zheng et al., 2022). The suspension in the bottle was shaken using the EZH-004C shaker (70°C, 145 r•min⁻¹). Three hours later, sodium carbonate (0.3 g) and 7.4 mol•L⁻¹ of isopropenyl acetate (16 mL) were added and the temperature was maintained at 40°C. After shaking with the oscillator (40°C, 145 r•min⁻¹) for 70 h, the reaction dispersion was filtered with a Whatman1004-047 paper. Isopropanol (60 mL) was used to purify the residual on the filter paper in triplicates. Then the residue was dried at 48°C. Seven hours later, jujube seed fiber treated with superfine-grinding and mix enzymolysis assisted by acetylation (JSF-SGEA) was obtained.

2.6 Determination of chemical constituent

The methods AOAC.955.04, AOAC.92.05, AOAC.924.05, and AOAC.920.39 were separately used to determine the contents of protein, fat, ash and moisture of JSF (AOAC, 2000). The contents of cellulose, lignin and hemicellulose were investigated using the procedures referring to Zhu et al. (2022). Moreover, AOAC.991.43 method was employed to determine the insoluble and total fiber contents, and soluble fiber content is the difference between total fiber content and insoluble fiber content (AOAC, 2000). Moreover, phenolic content determination was done with the Folin–Ciocalteu method (Cecilia et al., 2015).

2.7 Determination of particle size and color

JKFs were dispersed in distilled water (1: 25 g•mL⁻¹) and then analyzed with a WNNINER 336B nanometer size analysis system (Xinna particle Instrument Factory, Chengdu, China) (Zheng et al., 2022). The particle size was represented by Sauter mean diameter (D_{3,2}, μm) and the refractive index was 1.33. Moreover, the specific surface area (m²•kg⁻¹) of samples was read.

The color of JKF before and after the composite modifications was analyzed using a cr-10 spectrophotometer (Shenzhen Sanenshi Sci. and Tech. Co., Guangzhou, China). Color difference (ΔE) after the modifications were calculated with the Equation 1:

$$\Delta E = \sqrt{(L - L_0)^2 + (a - a_0)^2 + (b - b_0)^2} \quad (1)$$

where L , and L_0 are the lightness of JKF before and after the modifications; a and a_0 represent the redness of JKF before and after the modifications; and b and b_0 are representative of the yellowness of JKF before and after the modifications, respectively.

2.8 Changes in structure of JKF after modifications

2.8.1 Changes in microstructure

The changes in the microstructure of JKF after the composite modifications were determined using a Scanning Electron Microscopy system (SJM-JEOL-7200E, Electronics Co., Ltd., Showima city, Japan). The dried samples were fixed on the sample table by conductive adhesive. After spraying a 10-nm of gold, the samples on the table were photographed with a magnification of 2,000.

2.8.2 Fourier-transformed infrared spectroscopy

The infrared spectra of JKFs were drawn with a HS-FT-725 Fourier-transform infrared (FT-IR) spectrometer (Precision scientific instrument company, Shanghai, China). Dried KBr (0.2 g) was blended thoroughly with 4 mg of JKFs. Next, the mixed powder was pressed into a transparent sheet, and then analyzed by the spectrometer at scanning range of 4,000–400 cm⁻¹ and resolution of 4 cm⁻¹ (Zohaib et al., 2021).

2.9 Water adsorption and expansion capacities

In a graduated centrifugal tube, dried JKFs were dispersed in distilled water with a mass to volume ratio of 1: 15. The dispersion was placed at 25°C for 230 min. After centrifugation at 1,500 g for 25 min, the upper water was removed, and the wet JKFs were weighted (Zheng and Li, 2018). Oat β-D-glucan was used as the positive control. Water absorption capacity (WAC) was calculated as follows with the Equation 2:

$$WAC \left(g \cdot g^{-1} \right) = (W_w - W_d) / W_d \quad (2)$$

where W_w and W_d are representative of wet and dry weights of JKFs, respectively.

Moreover, dry JFKFs (3 g) were placed in a glass cylinder with plug and the volume was read (V_a , mL) (Zheng and Li, 2018). Next, 54 mL of distilled water was added and gently mixed for 3 min, and then the cylinder was placed at 25°C for 20 h. Afterward the volume of the wet JFKFs was read (V_w , mL), and water expansion ability (WEA) was calculated as follows with the Equation 3:

$$\text{WEA} \left(\text{mL} \cdot \text{g}^{-1} \right) = (V_w - V_a) / W_d \quad (3)$$

where W_d is the dry weight of JFKFs.

2.10 Viscosity

The viscosity of JFKFs (0.25 g·L⁻¹) was analyzed with the same procedure and parameters from Miehle et al. (2022) using a DV2T viscometer (Brookfield Company, Middleboro, Massachusetts, United States) at 35°C and shearing ratio of 500 s⁻¹, and oat β-D-glucan was used as the positive control.

2.11 Surface hydrophobicity

As per the method used by He et al. (2020), JFKF and the modified JFKFs (JKF-SGE, JKF-SGEA and JKF-SGEH) were dispersed into 0.1 mol·L⁻¹ of phosphate buffer (pH 7.4) for formulation solutions of different concentrations (20–500 μg·mL⁻¹). Next, 2.5 mL of the JFKFs solution was reacted with 25 μL of 1-anilino-8-naphthalenesulfonate (10 mmol·mL⁻¹) at 25°C for 2 min. Then the fluorescence intensity of the reaction solution was investigated with DOLOBF93 spectrophotometer (Lengguang Technology and Science Co. Ltd., Shanghai, China). The excitation and emission wavelengths were 390 and 470 nm, respectively. The regression curve between the fluorescent intensity of JFKFs' solution and their concentration was drawn, and the initial slope of the curve was defined as surface hydrophobicity.

2.12 Cation exchanging capacity

JKF and the modified JFKFs were separately dispersed into 0.1 mol·mL⁻¹ of HCl (1: 100, g/mL) and shaken in the HEZ-004C water bath oscillator at 25°C and 135 r·min⁻¹ for 48 h (Zheng and Li, 2018). After filtration on polyamide filter cloth (120 mesh), the filter residuum was continuously cleaned with dH₂O until there was no chloride ion in the washed solution, and then dried at 45°C for 270 min. Then the obtained JFKFs (1 g) was dispersed in 25 mL of NaCl (0.1 g·100 mL⁻¹), and titrated by 0.01 mol·mL⁻¹ of NaOH with phenolphthalein (2 mg·mL⁻¹, 200 μL) as the indicator. The volume of NaOH used was read until the pH value of the dispersion reached to 7.0. The number of milliequivalents per gram of JFKFs was defined as cation exchanging capacity (CEC) (mmol·g⁻¹), and β-D-glucan was used as comparison.

2.13 Adsorption capacity to oil

JKF (1 g, accurately weighed) and 10 mL of soybean oil were added into a graduated centrifuge tube, and then thoroughly mixed

at 275 r·min⁻¹ using a DTM-2500 vortex oscillator (Jitian Langyou Instrument Co., LTD, Changzhou, China) (Si et al., 2023). Five seconds later, the suspensions in the tube were left at 25 ± 1°C for 14 h, and centrifuged at 2,300× g for 15 min. The upper layer oil was discarded, and the residual pellet was accurately weighed and recorded. Oat β-D-glucan was used as comparison. The adsorption capacity to oil (ACO) was calculated according to the Equation 4:

$$\text{ACO} \left(\text{g} \cdot \text{g}^{-1} \right) = (W_w - W_D) / W_D \quad (4)$$

where W_w and W_D are representative of wet and dry weights of JFKFs, respectively.

2.14 Adsorption capacity of glucose

Before determination, JFKFs, JKF-SGE, JKF-SGEA, and JKF-SGEH (2 g) were separately suspended in 85% methanol solution (200 mL) to remove free sugar. The suspensions were heated at 50°C and shaken at 225 r·min⁻¹ for 75 min, and then filtered on nylon cloth with aperture of 150 meshes. The residues were dried at 45°C for 4 h, and desugared JFKFs were obtained. The adsorption capacity to glucose (ACG) of JFKFs was administrated referring to the same procedures from Zheng et al. (2022). The phenol-sulfuric acid method was employed to measure the original concentration of glucose before adsorption and the final glucose concentration after adsorption (Daou and Zhang, 2014), and β-D-glucan was used as comparison. ACG was calculated using the following Equation 5:

$$\text{ACG} \left(\mu\text{mol} \cdot \text{g}^{-1} \right) = (C_o - C_f) \times 400 / W \quad (5)$$

where C_o and C_f represent the original and final concentrations of glucose, respectively, and W is JFKFs' weight.

2.15 Statistics analysis

The mean and standard deviation for each data were obtained by duplicating the all experiments at least three times. Statistically differences were analyzed by analysis of variance (ANOVA) and Duncan test with the Ver.22.0 SPSS program (SPSS Inc., Chicago, America). The threshold for significant difference ($p < 0.05$) was 95%.

3 Results and discussion

3.1 Effects of different modifications on chemical component of JFKFs

The hydroxypropylation degree of JKF-SGEH was 2.59% ± 0.34%, suggesting that a part of hydroxyl groups in JKF have been replaced by hydroxypropyl groups. The modification process of JKF by superfine-grinding and mix enzymatic hydrolysis alone or combined with hydroxypropylation or acetylation is shown in Figure 1. Hydrogen bonds can be formed between adjacent hydroxyl groups on the cellulose chain. These hydrogen bonds are involved in the formation of the cellulose crystal structure, which can prevent the

penetration of water molecules (Zadeike et al., 2021). Superfine-grinding, mix enzymatic hydrolysis, or chemical modification can crack the hydrogen bonds and release more hydroxyl groups (Zheng et al., 2022). These free hydroxyl groups can be replaced by hydroxypropyl or acetyl group during hydroxypropylation or acetylation (Shaikh et al., 2019). Compared with hydrogen bond, hydroxypropyl group have higher hydrophilicity which probably improve the water solubility of JFK. The acetylated degree of JFK-SGEA was $1.87 \pm 0.13\%$, indicating that a part of hydrogen bonds in JFK have been replaced by acyl ester bonds which was conducive for the hydrophobicity of DFs (Gao et al., 2023). Moreover, these composite modification methods used in this study (superfine-grinding and mix enzymatic hydrolysis alone, and combined with acetylation or hydroxypropylation) have no obvious impact on the fat, protein and moisture contents ($p > 0.05$). By comparison, the soluble fiber content of JFK was remarkably improved after these composite modifications ($p < 0.05$). By contrast, these composite modification methods all remarkably enhanced the soluble fiber content of JFK ($p < 0.05$). Superfine-grinding can break the cell wall of fiber and increase its surface area, and cellulase, hemicellulase and Laccase can cause degradation of the glucosidic bonds, which both can release more hydrophilic groups and increase the soluble fiber content of JKE (Zheng and Li, 2018).

Moreover, the soluble fiber content of JFK-SGEH ($17.43 \pm 0.18 \text{ g} \cdot 100 \text{ g}^{-1}$) was much higher than JFK-SGE ($p < 0.05$), showing that hydroxypropylation significantly enhanced the effects of superfine-grinding and mix enzymatic hydrolysis to improve polarity of JFK. The introduced hydroxypropyl group had relatively high polarity (Kanwar et al., 2023). In comparison, the soluble content of JKE-SGEA was not different from that of JKE-SGE ($p > 0.05$). Previous studies showed that acyl ester bonds could increase the hydrophobicity of fibers (Nasseri et al., 2020; Zheng et al., 2022), therefore acetylation reduced the effect of superfine-grinding and mix enzymatic hydrolysis on polarity of JFK.

Additionally, the cellulose, hemicellulose and lignin contents of JFK were all decreased after the three modifications ($p < 0.05$), corresponding to their lower insoluble fiber content (Table 1). Cellulase, hemicellulase and Laccase can cause the degradation of cellulose, hemicellulose and lignin (Ma and Mu, 2016), resulting in

decreased insoluble fiber content and increased soluble fiber content. Furthermore, the soluble fiber contents of JFK, JFK-SGEH and JFK-SGEA ($13.64\text{--}17.43 \text{ g} \cdot 100 \text{ g}^{-1}$) were much higher than that of rice bran fiber ($3.03 \text{ g} \cdot 100 \text{ g}^{-1}$, Zadeike et al., 2021), coconut mesocarp fiber ($4.01 \text{ g} \cdot 100 \text{ g}^{-1}$, Zheng and Li, 2018), soybean hulls fiber ($1.76 \text{ g} \cdot 100 \text{ g}^{-1}$, Zhu et al., 2022), and sugarcane bagasse fiber ($3.12 \text{ g} \cdot 100 \text{ g}^{-1}$, Gil-López et al., 2019), highlighting their relatively high hydration properties.

Apart from that, the extractable polyphenol content of JFK was $3.46 \pm 0.22 \text{ mg} \cdot \text{g}^{-1}$, which was consistent with a previous study (Ji et al., 2020). The extractable polyphenol contents of JFK-SGE, JFK-SGEA and JFK-SGEH were all higher in comparison with that of JFK ($p < 0.05$), perhaps attributed to Laccase hydrolysis. Laccase caused degradation of lignin (polyphenol polymers) and thus significantly increased the extractable phenols (Zhang et al., 2022).

3.2 Effects of different modifications on particle size and color of JFK

The results in Table 2 show that all superfine-grinding and mix enzymatic hydrolysis, superfine-grinding and mix enzymatic hydrolysis combined with acetylation or hydroxypropylation all increased the surface area of JFK and reduced its particle size ($p < 0.05$). Mix enzymatic hydrolysis and superfine-grinding both can cause the breakdown of fiber cell wall and degradation of polysaccharide chains (Liu et al., 2021), resulting in reduction of JFK's particle size. The surface area of JFK-SGEH ($142.53 \pm 3.14 \text{ m}^2 \cdot \text{kg}^{-1}$) was higher than other JFKs, and its particle size ($61.54 \pm 1.75 \mu\text{m}$) was lower than other JFKs ($p < 0.05$). The touching chance between JFK and oil or sugar molecules will be increased as surface area became larger, and the functional properties of JFK will be improved as consequence (Hua et al., 2019).

Moreover, JFK-SGE, JFK-SGEH, and JFK-SGEA all showed lower L' value but higher a' and b' values in comparison with JFK ($p < 0.05$), indicating these composite modifications have reduced the brightness of JFK and increased its redness and yellowness. During superfine-grinding, hydroxypropylation and acetylation, several procedures such as high-speed shear force, heating, and strong alkaline treatment

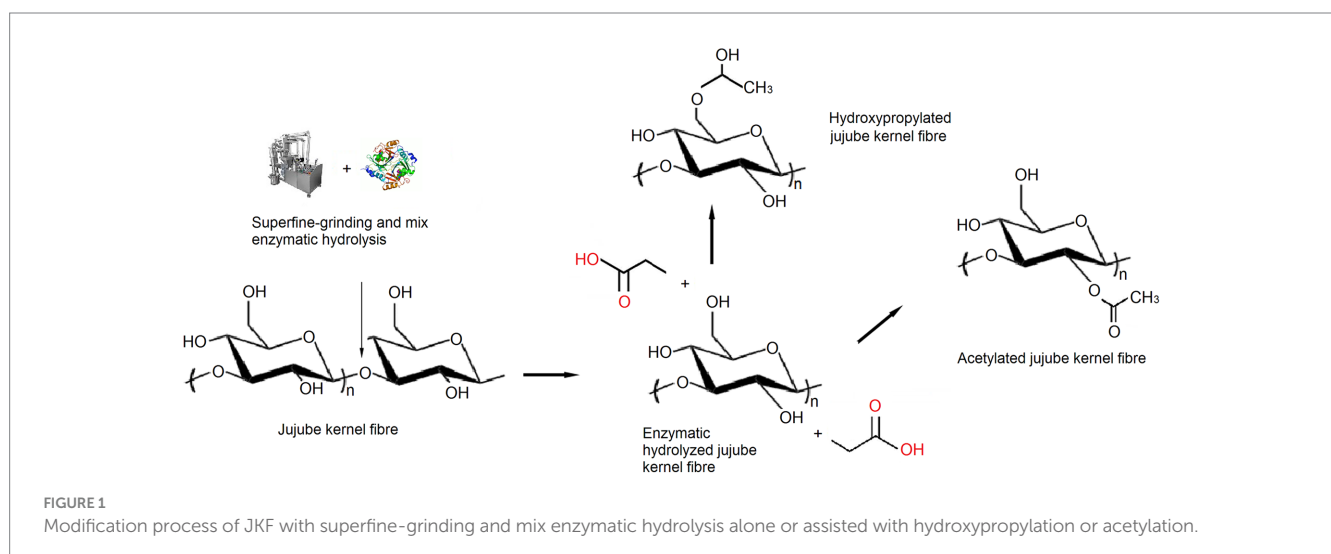


TABLE 1 Proximate compositions of jujube kernel fiber (JKF), JKF modified by superfine-grinding and mix enzymatic (cellulase, hemicellulase, and Laccase) hydrolysis (JKF-SGE), JKF treated by superfine-grinding, and mix enzymatic hydrolysis combined with hydroxypropylation (JKF-SGEH), and JKF modified by superfine-grinding and mix enzymatic hydrolysis combined with acetylation (JKF-SGEA).

Constituent	Jujube kernel	JKF	JKF-SGE	JKF-SGEH	JKF-SGEA
Moisture (g•100 g ⁻¹)	5.25 ± 0.47a	6.38 ± 0.11a	5.37 ± 0.09a	4.73 ± 0.17a	5.12 ± 0.15a
Fat (g•100 g ⁻¹)	2.74 ± 0.25a	1.93 ± 0.27b	1.24 ± 0.05b	1.12 ± 0.07b	1.01 ± 0.06b
Ash (g•100 g ⁻¹)	0.81 ± 0.11b	0.95 ± 0.04b	1.51 ± 0.06a	1.64 ± 0.11a	1.41 ± 0.15a
Protein (g•100 g ⁻¹)	0.87 ± 0.09a	0.38 ± 0.06a	0.45 ± 0.03a	0.22 ± 0.01a	0.62 ± 0.06a
Total fiber (g•100 g ⁻¹)	87.36 ± 2.74b	89.76 ± 2.56a	91.36 ± 2.69a	91.75 ± 2.27a	90.64 ± 3.73a
Insoluble fiber (g•100 g ⁻¹)	81.87 ± 1.65a	83.44 ± 3.43a	77.72 ± 3.48b	74.32 ± 3.33a	76.64 ± 2.57b
Soluble fiber (g•100 g ⁻¹)	5.49 ± 0.24c	6.32 ± 0.33c	13.64 ± 1.42b	17.43 ± 0.18a	14.00 ± 1.22b
Extractable polyphenols (mg g ⁻¹)	3.46 ± 0.22d	5.82 ± 0.37c	12.65 ± 0.16a	10.45 ± 0.48b	10.07 ± 0.45b
Cellulose (g•100 g ⁻¹)	40.83 ± 1.64a	41.82 ± 1.43a	34.27 ± 1.25b	33.67 ± 0.16b	31.91 ± 1.02b
Hemicellulose (g•100 g ⁻¹)	24.25 ± 0.39a	24.67 ± 0.78a	17.58 ± 0.50b	18.15 ± 0.41b	18.05 ± 0.67b
Lignin (g•100 g ⁻¹)	24.37 ± 3.14a	26.17 ± 3.27a	14.34 ± 0.78b	10.02 ± 0.44c	8.39 ± 0.47c

Different small letters (a–e) in the same line meant significant difference ($p < 0.05$).

TABLE 2 Particle size distribution, color, and adsorption properties of JKF, JKF-SGE, JKF-SGEH, and JKF-SGEA with β -D-glucan as comparison.

Properties	JKF	JKF-SGE	JKF-SGEH	JKF-SGEA	β -D-Glucan
D _{3,2} (μ m)	132.94 ± 3.62a	73.35 ± 4.27b	61.54 ± 1.75c	68.72 ± 2.47b	49.08 ± 1.75d
Surface area (m ² •kg ⁻¹)	51.46 ± 1.28c	129.22 ± 5.68b	142.53 ± 3.14a	127.46 ± 2.37b	152.67 ± 5.75a
L*	62.27 ± 1.02a	49.65 ± 1.49b	46.76 ± 2.26b	42.58 ± 4.67c	ND
a*	16.36 ± 0.34b	15.75 ± 0.46a	17.15 ± 0.43a	17.85 ± 0.35a	ND
b*	27.64 ± 0.47c	29.10 ± 1.99b	27.98 ± 1.33b	26.94 ± 1.74a	ND
ΔE	Control	12.72c	15.53b	19.76a	ND
Water absorption capacity (g•g ⁻¹)	4.46 ± 0.30c	7.73 ± 0.28b	9.57 ± 0.34a	6.47 ± 0.49b	3.73 ± 0.26c
Water expansion ability (mL•g ⁻¹)	4.20 ± 0.10c	6.00 ± 0.20b	7.60 ± 0.10a	5.80 ± 0.20b	4.94 ± 0.20c
Viscosity (cP)	8.42 ± 0.15d	11.27 ± 0.15c	14.54 ± 0.22b	14.33 ± 0.33b	18.25 ± 1.07a
Surface hydrophobicity	36.50 ± 3.44b	28.65 ± 2.59c	22.42 ± 1.62d	43.57 ± 3.36a	25.77 ± 2.31d
Cation exchange capacity (μ mol•g ⁻¹)	19.26 ± 1.19d	26.42 ± 1.77c	40.82 ± 3.71a	32.88 ± 3.47b	25.00 ± 1.05c
Adsorption ability to oil (g•g ⁻¹)	1.56 ± 0.21c	1.32 ± 0.07c	2.77 ± 0.28b	4.47 ± 0.34a	3.26 ± 0.22ab
Adsorption capacity to glucose (μ mol•g ⁻¹)	15.20 ± 0.29c	20.73 ± 1.77b	29.61 ± 2.43a	10.76 ± 0.36d	23.51 ± 2.60b

Different small letters (a–d) in the same line meant significant difference ($p < 0.05$).

may cause caramelization reaction between fiber molecules, decreasing the brightness of JKF (Nasseri et al., 2020). Moreover, the introduced hydroxypropyl and acetyl groups can cause browning reaction under alkaline conditions (Zheng et al., 2022), leading to an increase in a^* and b^* values of JKF. Brown color may be not conducive to the utilization of JKFs in food industry.

3.3 Effects of different modifications on structure of JKF

3.3.1 Changes in microstructure

As shown in Figure 2A, JKF offered a relatively smooth microstructure surface with some fragments. By contrast, JKF-SGE, JKF-SGEA and JKF-SGEC all showed irregular and fragmented

microstructures with a large amount of pores (Figures 2B–D). Superfine-grinding can breakdown the cell wall of JKF, and mix enzymatic hydrolysis can crack the glucosidic bonds of JKF (Zadeike et al., 2021; Qin et al., 2023), resulting in a honeycomb microstructure of JKF-SGE (Figure 2B). After hydroxypropylation and acetylation, the processing such as heating, strong alkaline treatment, and oxidation reaction bring changes in structure of JKF (Zheng et al., 2022), leading to a microstructure with larger holes or more fragments (Figures 2C,D). These results show that the three composite modifications all changed the structure of JKF. Moreover, the fragmented and porous microstructures of JKF-SGE, JKF-SGEA, and JKF-SGEC were in accordance with their larger surface area and smaller particle sizes (Table 2). Moreover, fibers with porous microstructure always exhibit high sorption capacities on oil, sugar and heavy metals (Kanwar et al., 2023).

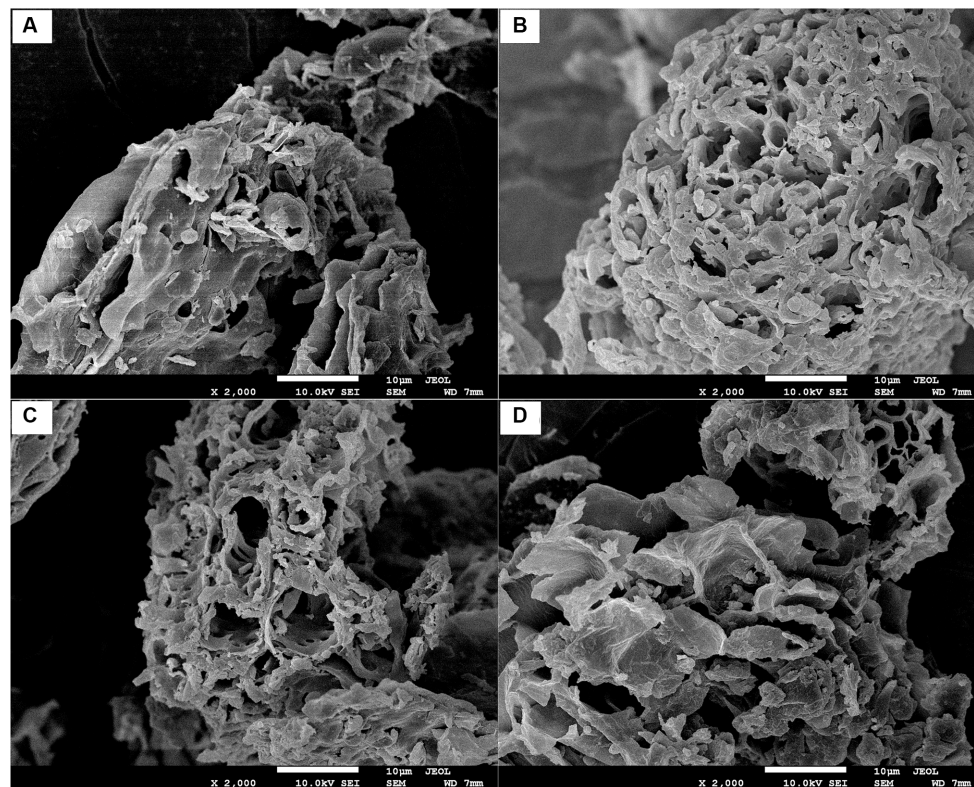


FIGURE 2

Scanning electron micrographs of JKF (A), JKF-SGE (B), JKF-SGEA (C), and JKF-SGEH (D) with a magnification of 2,000 \times , at 1 μ m. JKF, Jujube kernel fiber; JKF-SGE, JKF modified by superfine-grinding and mix enzymatic (cellulase, hemicellulase and Laccase) hydrolysis; JKF-SGEA, JKF modified by superfine-grinding and mix enzymatic hydrolysis combined with acetylation; and JKF-SGEH, JKF treated by superfine-grinding and mix enzymatic hydrolysis combined with hydroxypropylation.

3.3.2 Ft-IR

The FT-IR spectra and principal functional groups of JKF, JKF-SGE, JKF-SGEA, and JKF-SGEH are shown in Figure 3 and Table 3. There are visible differences between these functional groups, indicating that the composite modification caused structural change. Compared with the spectrum of JKF, the peak at 786 cm^{-1} (representing the stretching and flexion of C–O) transferred to 782, 779, and 777 cm^{-1} in the spectra of JKF-SGE, JKF-SGEA and JKF-SGEH, respectively, due to the breakdown of β -glycosidic bond as a sequence of superfine-grinding and enzymolysis (Hua et al., 2019; Djordjević et al., 2021). Obvious red-shift happened on the peak located at wavenumber of around 3,460 cm^{-1} (indicative of the stretching of O–H) in the spectra of JKF-SGE, JKF-SGEA, and JKF-SGEH, suggesting that superfine-grinding and enzymolysis, superfine-grinding and enzymolysis assisted with acetylation or hydroxypropylation all have changed the hydrogen bonds of JKF (Hazarika and Sit, 2016; Tapia-Hernández et al., 2019b). As shown in Figure 3, the hydrogen bonds between fiber chains were partly cracked and replaced by acetyl or hydroxypropyl groups, corresponding to the shift on the peak at around 3,460 cm^{-1} . Moreover, the peaks at wavenumbers of 1,632 and 1,110, 1,378 cm^{-1} (separately indicative of the asymmetric bend of acetyl group, C–H, and –C=O, respectively, Gil-López et al., 2019) in the spectrum of JKF separately presented at wavenumbers of 1,622, 1,107, and 1,369 cm^{-1} in the spectrum of JKF-SGEA, demonstrating that acyl ester groups have been introduced

into JKF molecules after acetylation. Additionally, compared with the spectrum of JKF, the spectrum of JKF-SGEH has two new peaks appearing at wavenumber of 913 and 2,734 cm^{-1} (indicative of the stretching and flexion of C–O and C–H, respectively), and the peak at 2850 cm^{-1} transferred to 2,845 cm^{-1} (indicative of the flexion of C–H), which is attributed to the introduction of hydroxypropyl group after hydroxypropylation (Tapia-Hernández et al., 2019b; Akinterinwa et al., 2020). Previous studies shown that superfine-grinding, acetylation and hydroxypropylation all could influence the structure of fibers via changing their chemical bonds (Shaikh et al., 2019; Zheng et al., 2022).

3.4 Water adsorption and expansion capacities

High water adsorption capacity (WAC) and water expansion capacity (WEA) mean fibers can rapidly absorb water and expand, which is helpful to the adsorption of oil and sugar on fibers (Miehle et al., 2022). The results in Table 2 show that JKF-SGE, JKF-SGEA and JKF-SGEH showed higher WAC and WEA than JKF and oat β -D-glucan ($p < 0.05$), suggesting that superfine-grinding and mix enzymatic hydrolysis, superfine-grinding and mix enzymatic hydrolysis combined with hydroxypropylation or acetylation all enhanced the WAC and WEA of JKF, mainly attributed to the

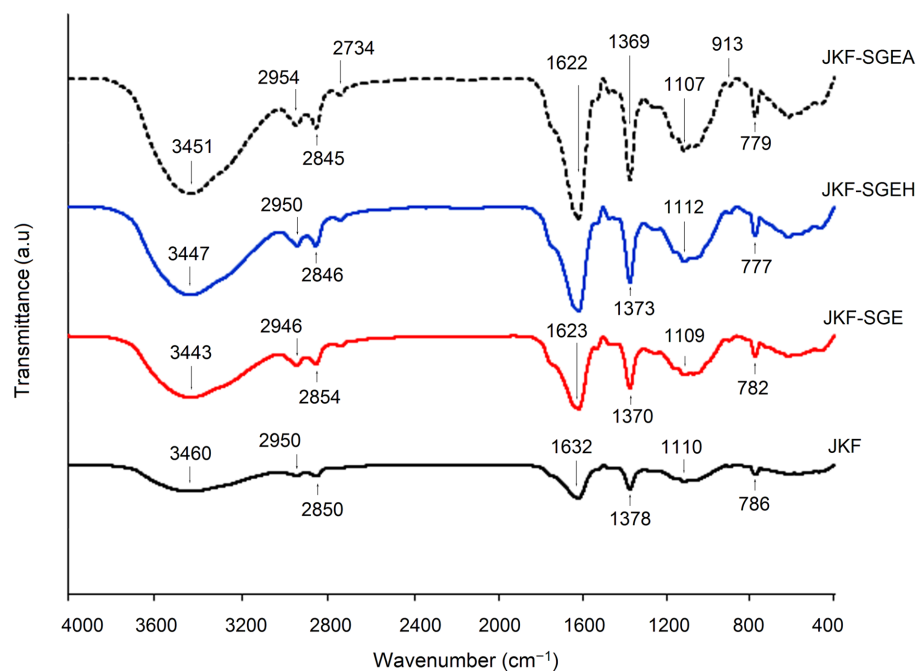


FIGURE 3
Fourier-transformed infrared spectra of JKF, JKF-SGE, JKF-SGEH, and JKF-SGEA.

TABLE 3 Principal functional groups of the JKF, JKF-SGE, JKF-SGEH, and JKF-SGEA.

Functional groups	Type of vibration	Wavenumber (cm ⁻¹)			
		JKF	JKF-SGE	JKF-SGEH	JKF-SGEA
O-H	Stretching	3,460	3,443	347	3,451
C-H	Stretching	2,950	2,946	2,950	2,954
C-H	Stretching	2,850	2,854	2,846	2,845
					2,734
C-O-C	Asymmetric bend	1,632	1,623	1,625	1,622
C-C/C-H	Stretching	1,378	1,370	1,373	1,369
-C=O	Stretching and flexion	1,110			1,107
C-O	Stretching and flexion				913
C-O	Stretching and flexion	786	782	777	779

improvement of soluble fiber content and the changes in surface area and microstructure of JKF after these modifications. Higher soluble fiber content (Table 1) means that JKF-SGE, JKF-SGEA and JKF-SGEH have stronger affinity with water molecules than JKF. Moreover, the larger surface area and the microstructures with a lot of holes and fragment (Figures 2B,C; Table 2) can ensure that JKF-SGE, JKF-SGEA and JKF-SGEH have more touching chance and stronger interactions with water molecules (Liu et al., 2021).

JKF-SGEH exhibited the highest WAC (9.57 g•g⁻¹) and the largest expansion volume (7.60 mL•g⁻¹) among these JKFs, corresponding to its highest soluble fiber content (17.43 ± 0.18 g•100 g⁻¹), evidencing that superfine-grinding and mix enzymatic hydrolysis combined with hydroxypropylation was more effective to improve the water adsorption and expansion capacities of JKF than superfine-grinding and mix enzymatic hydrolysis alone. The main reason was that after

hydroxypropylation, the introduced hydroxypropyl groups can significantly increase the polarity of JKF, and enhance the steric hindrance between its polysaccharide chains which both play an important role in WAC and WEA of fibers (Shaikh et al., 2019). Moreover, JKF-SGEA also offered higher WAC and WEA than JKF ($p < 0.05$), but these values were not significantly different from that of JKF-SGE ($p > 0.05$), probably due to the introduced acyl ester groups had relatively high hydrophobicity rather than hydrophilicity (Nasser et al., 2020; Feng et al., 2024).

3.5 Viscosity

Increment of viscosity of DFs indicates that DFs have stronger ability to increase the viscosity of digestive juice and delay the

diffusion and absorption of sugar and oil, thereby improving the hypoglycemic and hypolipidemic effects of DFs (Peerajit et al., 2022). Superfine-grinding and mix enzymatic hydrolysis combined with hydroxypropylation or acetylation both exhibited more effective improvement in viscosity of JKE than superfine-grinding and mix enzymatic hydrolysis alone, for JKF-SGEH and JKF-SGEA both showed higher viscosity (16.33–16.54 cP) than JKF-SGE and JKF ($p < 0.05$). It has been evidenced that viscosity of DFs belongs to hydration and rheological properties which are dependent on the affinity of DFs with water molecules, molecular mass, conformation of polysaccharide chains, and environment factors (such as pH, temperature, and ionic strength) (Liu et al., 2021; Zheng et al., 2023). Therefore, the higher soluble fiber content, WEA and WSC, larger surface area, and the more fragment and the microstructures with a lot of holes and fragment (Tables 1, 2 and Figures 2C,D) all can improve the interactions of JKF with water molecules, and thus contributed to the high viscosity of JKF-SGEH and JKF-SGEA. The viscosity of JKF-SGEH, JKF-SGEA and JKE-SGE was lower than that of β -D-glucan (18.25 ± 1.07 cP), but was higher than that of millet bran dietary fiber and coconut cake dietary fiber (Zheng and Li, 2018; Zheng et al., 2022), indicating their higher hypoglycemic and hypolipidemic effects.

3.6 Surface hydrophobicity

Surface hydrophobicity was positively correlated with the chemical adsorption of lipids on fibers. The result in Table 2 showed the surface hydrophobicity of JKF-SGE and JKF-SGEH was both lower than that of JKF ($p < 0.05$), highlighting superfine-grinding and enzymolysis alone, superfine-grinding and enzymolysis combined with hydroxypropylation both reduced hydrophobicity of JKF. Superfine-grinding and mix enzymatic hydrolysis caused the glucosidic bonds degradation of JKF and released groups with higher hydrophilicity (Backes et al., 2021; Zohaib et al., 2021), and the introduced hydroxypropyl groups increased the hydrophilicity of JKF (Zheng et al., 2022), which were all contributed to the lower surface hydrophobicity of JKF-SGE and JKF-SGEH. In contrast, the surface hydrophobicity of JKF-SGEA was much higher compared with that of JKF ($p < 0.05$), for the introduced acyl ester group after acetylation had relatively high hydrophobicity (Zheng et al., 2022). Previous studies found that acetylation improved surface hydrophobicity of starch and oil palm empty fruit bunch fibers, too (Nasseri et al., 2020; Asadpour et al., 2021). Additionally, both JKF-SGEA and JKF-SGEH showed higher surface hydrophobicity than that of oat β -D-glucan ($p < 0.05$, Table 2), indicating their potential higher interaction with oil (Ellefsen et al., 2023).

3.7 Cation exchanging capacity

As shown in Table 2, the cation exchanging capacity (CEC) of JKF-SGE, JKF-SGEA and JKF-SGEH was all higher than that of JKF ($p < 0.05$). It was shown that the CEC of fibers depends on their chemical compositions with negative polarity. Some special chemical groups such as free hydroxyl, carboxyl and phenolic acid groups can significantly improve the affinity of fibers with cation ions (Gil-López et al., 2019). The introduced acyl ester and hydroxypropyl groups

remarkably increased the negative charge of JKF (Zheng et al., 2022), and more functional groups of JKF were exposed after superfine-grinding and enzymolysis (Zadeike et al., 2021), which all enhanced the combination of JKF with cation ions and improved its CEC. Besides, the higher extractable polyphenols content (10.07 – 12.65 $\text{mg}\cdot\text{g}^{-1}$, Table 1), bigger surface area (127.46 – 142.53 $\text{m}^2\cdot\text{kg}^{-1}$, Table 2), and more fragmented and the microstructures with a lot of holes and fragment (Figures 2B–D) were all contributed to the high CEC of JKF-SGE, JKF-SGEA and JKF-SGEC. A bigger surface area can increase the touching chance of JKF with cation ions, while fibers of porous microstructure easily capture cation ions (Zhu et al., 2022).

Furthermore, JKF-SGEH offered the highest CEC (40.82 ± 3.71 $\mu\text{mol}\cdot\text{g}^{-1}$) among these JKFs and β -D-glucan ($p < 0.05$). Apart from the porous microstructure (Figure 2C), the large surface area (142.53 $\text{m}^2\cdot\text{kg}^{-1}$) and high extractable polyphenol content (10.45 ± 0.48 $\text{mg}\cdot\text{g}^{-1}$, Table 1) contributed to the high CEC of JKF-SGEH. Moreover, hydroxypropylation can increase the free hydroxyl group content of fibers which play an important role in CEC (Kanwar et al., 2023), thereby enhancing the chelation of JKF with cation ions. The CEC of JKF-SGEA was higher than that of JKF and JKF-SGE ($p < 0.05$), mainly due to the improvement of negative charge as a consequence of the introduced acetyl ester groups. Additionally, the CEC of JKF-SGEH was higher than that of rice bran fiber (35.2 $\mu\text{mol}\cdot\text{g}^{-1}$, Zadeike et al., 2021) and soybean bran fiber (35.2 $\mu\text{mol}\cdot\text{g}^{-1}$, Zhu et al., 2022), highlighting their potential usage for treat cation ions in food or drinking water.

3.8 Adsorption capacity of oil on JKFs

JKF showed a poor oil adsorption ability (OAA) (1.56 ± 0.21 $\text{g}\cdot\text{g}^{-1}$, Table 2), which was consistent with the result of Xia et al. (2023). JKF-SGEA and JKF-SGEH both offered a stronger adsorption affinity to oil (2.77 – 4.47 $\text{g}\cdot\text{g}^{-1}$) than JKF ($p < 0.05$); while the OAA of JKF-SGE was lower than JKF's ($p > 0.05$), evidencing that acetylation or hydroxypropylation improved the OAA of JKF, but superfine-grinding and mix enzymatic hydrolysis reduced it. The main reason for the high OAA of JKF-SGEA was that the introduced acyl ester groups after acetylation significantly increased the surface hydrophobicity of JKF (Table 2) and thus enhanced the OAA of JKF. Moreover, the increment in surface area and WEC (Table 2), and the microstructure with a lot of holes and fragment (Figure 2C) after acetylation were all helpful to the adsorption of oil on JKF-SGEA (Sang et al., 2022). Asadpour et al. (2021) also found that the OAA of oil palm empty fruit bunch fiber can be significantly improved by acetylation. Other substances with porous structure such as active carbon exhibit excellent oil-adsorption capacity, too (Campos et al., 2018). With respect to JKF-SGEH, the high OAA was mainly attributed to the larger surface area, higher WEC, and the microstructure with a lot of holes and fragment (Table 2; Figure 2D). A higher WEC indicates that DFs have a larger expansion volume in wastewater which was conducive for the adsorption of oil on DFs (Kanwar et al., 2023). By contrast, although with the bigger WEC and the microstructure with a lot of holes and fragment (Table 2; Figure 2B), JKF-SGE showed a poor OAA, mainly due to its lower surface hydrophobicity (28.65 ± 2.59 , Table 2). It has been shown that fibers can adsorb oil via chemical adsorption mechanism or physical adsorption patterns (Si et al., 2023). The results in the current study demonstrated that oil molecules can be adsorbed

by JKF-SGE, JKF-SGEA or JKF-SGEH via both chemical and physical adsorption mechanisms. In addition, the OAA of JKF-SGEA and JKF-SGEH ($2.77\text{--}4.47\text{ g}\cdot\text{g}^{-1}$) was nearly equal to that of β -D-glucan which has been found to have good lipid-lowering effect (Ellefsen et al., 2023), indicating their potential applications as ingredients of hypolipidemic foods.

3.9 Adsorption capacity of glucose

For hyperglycemic patient, it is important to reduce blood sugar to the normal range of $3.9\text{--}6.1\text{ mmol}\cdot\text{L}^{-1}$ (Hua et al., 2019). The adsorption capacity of glucose (ACG) of JKF was higher than that of JKF-SGEA but lower than that of JKF-SGE and JKF-SGEH ($p < 0.05$, Table 2), showing that superfine-grinding and mix enzymatic hydrolysis alone or combined with hydroxypropylation both improved the ACG of JKF, while acetylation decreased it. Miehle et al. (2022) and Zheng et al. (2022) demonstrated that the adsorption of fibers to glucose via chemical affinity or physical adsorption, and increase in hydrophilicity and surface area, and a more porous microstructure all can enhance the adsorption of glucose on fibers. Therefore, the highest soluble fiber content (corresponding to high hydrophilicity) ($17.43 \pm 0.18\text{ g}\cdot 100\text{ g}^{-1}$, Table 1), largest surface area ($142.53 \pm 3.14\text{ m}^2\cdot\text{kg}^{-1}$, Table 2), and the microstructure with a lot of holes and fragment (Figure 2D) were all responsible for the highest ACG of JKF-SGEH ($29.61\text{ }\mu\text{mol}\cdot\text{g}^{-1}$). Alternatively, the introduced acyl ester groups increased the surface hydrophobicity of JKF and thus decreased the interactions between JKF and glucose, resulting in a low ACG of JKF-SGEA. Moreover, the ACG of JKF-SGE was lower than that of JKF-SGEH, evidencing that hydroxypropylation can significantly increase the improvement effect of superfine-grinding and mix enzymatic hydrolysis in ACG of JKF. In addition, JKF-SGEH showed a higher ACG than that of β -D-glucan (a well-known blood sugar-lowering polysaccharide, Ellefsen et al., 2023), highlighting its potential usage as ingredient of hypoglycemic foods.

4 Conclusion

Three composite modifications including superfine-grinding and mix enzymatic hydrolysis, superfine-grinding and mix enzymolysis separately combined with acetylation and hydroxypropylation all lowered the particle size and changed the microstructure of JKF, and improved its soluble fiber and extractable polyphenol contents, water adsorption and expansion abilities, and cation exchange capacity ($p < 0.05$), but lowered its brightness. Compared with superfine-grinding and mix enzymolysis alone, superfine-grinding and mix enzymolysis combined with acetylation more effectively enhanced the surface hydrophobicity and the adsorbing ability toward oil of JKF; meanwhile JKF modified by superfine-grinding and mix enzymatic

hydrolysis combined with hydroxypropylation exhibited the highest hydration properties, cation exchange capacity and adsorption capacity to glucose, and it has potential as ingredient of hypoglycemic foods. The JKF modified by superfine-grinding and mix enzymatic hydrolysis combined with acetylation can be used as ingredient of hypolipidemic foods. However, the hypolipidemic and hypoglycemic effects of these modified JKFs need further works. The modifications of jujube kernel fiber (JKF) improved the physicochemical and structural properties to obtain a more techno-functional material for its potential use in the food industry.

Data availability statement

The original contributions presented in the study are included in the article/supplementary material, further inquiries can be directed to the corresponding author.

Author contributions

JZ: Conceptualization, Funding acquisition, Investigation, Project administration, Writing – original draft. ZY: Methodology, Validation, Writing – review & editing.

Funding

The author(s) declare that financial support was received for the research, authorship, and/or publication of this article. This research was funded by the Natural Science Foundation of Shanxi Province, China (202303021211106), and the Science and Technology Achievement Transformation Guidance Special Project of Shanxi Province, China (202104021301051).

Conflict of interest

The authors declare that the research was conducted in the absence of any commercial or financial relationships that could be construed as a potential conflict of interest.

Publisher's note

All claims expressed in this article are solely those of the authors and do not necessarily represent those of their affiliated organizations, or those of the publisher, the editors and the reviewers. Any product that may be evaluated in this article, or claim that may be made by its manufacturer, is not guaranteed or endorsed by the publisher.

References

- Agrawal, P., Singh, T., Pathak, D., and Chopra, H. (2023). An updated review of Ziziphus jujube: major focus on its phytochemicals and pharmacological properties. *Pharmacol. Res. Mod. Chin. Med.* 8:100297. doi: 10.1016/j.prmcm.2023.100297
- Akinterinwa, A., Oladele, E., Adebayo, A., Gurgur, E., Iyanu, O. O., and Ajayi, O. (2020). Cross-linked-substituted (esterified/etherified) starch derivatives as aqueous heavy metal ion adsorbent: a review. *Water Sci. Technol.* 82, 1–26. doi: 10.2166/wst.2020.332
- Al-Khalili, M., Al-Habsi, N., Al-Alawi, A., Al-Subhi, L., Myint, M. T. Z., Al-Abri, M., et al. (2021). Structural characteristics of alkaline treated fibers from date-pits: residual and precipitated fibers at different pH. *Bioact. Carbohydr. Diet. Fibre* 25:100251. doi: 10.1016/j.bcdf.2020.100251
- AOAC. (2000). *Official methods of analysis*. Washington, DC: Association of Official Analytical Chemists.

- Asadpour, R., Yavari, S., Kamyab, H., Ashokkumar, V., Chelliapan, S., and Yuzir, A. (2021). Study of oil sorption behaviour of esterified oil palm empty fruit bunch (OPEFB) fibre and its kinetics and isotherm studies. *Environ Technol. Inno.* 22:101397. doi: 10.1016/j.eti.2021.101397
- Backes, E., Kato, C. G., Corrêa, R. C. G., Moreira, R. F. P. M., Peralta, R. A., Barros, L., et al. (2021). Laccases in food processing: current status, bottlenecks and perspectives. *Trends Food Sci. Tech.* 115, 445–460. doi: 10.1016/j.tifs.2021.06.052
- Bai, L., Zhang, H., Liu, Q., Zhao, Y., Cui, X., Guo, S., et al. (2016). Chemical characterization of the main bioactive constituents from fruits of *Ziziphus jujube*. *Food Funct.* 7, 2870–2877. doi: 10.1039/C6FO00613B
- Cai, W., Tang, F., Guo, Z., Zhang, Q., Zhao, X., Ning, M., et al. (2020). Effects of pretreatment methods and leaching methods on jujube wine quality detected by electronic senses and HS-SPME-GC-MS. *Food Chem.* 330:127330. doi: 10.1016/j.foodchem.2020.127330
- Campos, A., Sena Neto, A. R., Rodrigues, V. B., Luchesi, B. R., Mattoso, J. M., and Marconcini, J. M. (2018). Effect of raw and chemically treated oil palm mesocarp fibers on thermoplastic cassava starch properties. *Ind. Crop. Prod.* 124, 149–154. doi: 10.1016/j.indcrop.2018.07.075
- Cecilia, V. V., María, G. V. R., Carolina, A. R., Jorge, L. C., Teresa, G.-G., Roberto, A., et al. (2015). Total phenolic compounds in milk from different species. Design of an extraction technique for quantification using the Folin-Ciocalteu method. *Food Chem.* 176, 480–486.
- Daou, C., and Zhang, H. (2014). Functional and physiological properties of total, soluble, and insoluble dietary fibers derived from defatted rice bran. *J Food Sci. Tech.* 51, 3878–3885. doi: 10.1007/s13197-013-0925-y
- Djordjević, M., Šereš, Z., Maravić, N., Šćiban, M., Šoronja-Simović, D., and Djordjević, M. (2021). Modified sugar beet pulp and cellulose-based adsorbents as molasses quality enhancers: assessing the treatment conditions. *LWT-Food Sci. Technol.* 150:111988. doi: 10.1016/j.lwt.2021.111988
- Ellefsen, C. F., Lindstad, L., Kalu, L. J., Aachmann, F. L., Hiorth, M., and Samuelsen, A. B. C. (2023). Investigation of the structural and immunomodulatory properties of alkali-soluble β -glucans from *Pleuroutus eryngii* fruiting bodies. *Carbohydr. Polym.* 322:121367. doi: 10.1016/j.carbpol.2023.121367
- Elleuch, M., Bedigian, D., Roiseux, O., Besbes, S., Blecker, C., and Attia, H. (2011). Dietary fibre and fibre-rich by-products of food processing: Characterisation, technological functionality and commercial applications: A review. *Food Chem.* 124, 411–421.
- Feng, X., Ameer, K., Jiang, G., and Ramachandiraiah, K. (2024). Effects of extraction methods on the structural characteristics and functional properties of dietary fiber extracted from papaya peel and seed. *Front. Sustain. Food Syst.* 8:1340961. doi: 10.3389/fsufs.2024.1340961
- Gao, K., Liu, T., Zhang, Q., Wang, Y., Song, X., Luo, X., et al. (2023). Stabilization of emulsions prepared by ball milling and cellulase treated pomelo peel insoluble dietary fiber: integrity of porous fiber structure dominates the stability. *Food Chem.* 440:138189. doi: 10.1016/j.foodchem.2023.138189
- Gil-López, D. I. L., Lois-Correa, J. A., Sánchez-Pardo, M. E., Domínguez-Crespo, M. A., Torres-Huerta, A. M., Rodríguez-Salazar, A. E., et al. (2019). Production of dietary fibers from sugarcane bagasse and sugarcane tops using microwave-assisted alkaline treatments. *Ind. Crop. Prod.* 135, 159–169. doi: 10.1016/j.indcrop.2019.04.042
- Hazarika, B. J., and Sit, N. (2016). Effect of dual modification with hydroxypropylation and cross-linking on physicochemical properties of taro starch. *Carbohydr. Polym.* 140, 269–278. doi: 10.1016/j.carbpol.2015.12.055
- He, K., Li, Q., Li, Y., Li, B., and Liu, S. (2020). Water-insoluble dietary fibers from bamboo shoot used as plant food particles for the stabilization of O/W Pickering emulsion. *Food Chem.* 310:125925. doi: 10.1016/j.foodchem.2019.125925
- Hua, M., Lu, J., Qu, D., Liu, C., Zhang, L., Li, S., et al. (2019). Structure, physicochemical properties and adsorption function of insoluble dietary fiber from ginseng residue: a potential functional ingredient. *Food Chem.* 286, 522–529. doi: 10.1016/j.foodchem.2019.01.114
- Ji, X., Hou, C., Yan, Y., Shi, M., and Liu, Y. (2020). Comparison of structural characterization and antioxidant activity of polysaccharides from jujube (*Ziziphus jujuba* mill.) fruit. *Int. J. Biol. Macromol.* 149, 1008–1018. doi: 10.1016/j.ijbiomac.2020.02.018
- Ji, R., Zhang, X., Liu, C., Zhao, W., Han, X., and Zhao, H. (2024). Effects of extraction methods on the structure and functional properties of soluble dietary fiber from blue honeysuckle (*Lonicera caerulea* L.) berry. *Food Chem.* 431:137135. doi: 10.1016/j.foodchem.2023.137135
- Kanwar, P., Yadav, R. B., and Yadav, B. S. (2023). Cross-linking, carboxymethylation and hydroxypropylation treatment to sorghum dietary fiber: effect on physicochemical, micro structural and thermal properties. *Int. J. Biol. Macromol.* 233:123638. doi: 10.1016/j.ijbiomac.2023.123638
- Liu, Y., Yi, S., Ye, T., Leng, Y., Hossen, M. A., Sameen, D. E., et al. (2021). Effects of superfine-grinding and homogenization on physicochemical properties of okara dietary fibers for 3D printing cookies. *Ultrason. Sonochem.* 77:105693. doi: 10.1016/j.ultsonch.2021.105693
- Ma, M., and Mu, T. (2016). Modification of deoiled cumin dietary fiber with laccase and cellulase under high hydrostatic pressure. *Carbohydr Polyme.* 136, 87–94. doi: 10.1016/j.carbpol.2015.09.030
- Miehle, E., Hass, M., Bader-Mittermaier, S., and Eisner, P. (2022). The role of hydration properties of soluble dietary fibers on glucose diffusion. *Food Hydrocolloid.* 131:107822. doi: 10.1016/j.foodhyd.2022.107822
- Nasserri, R., Ngunjiri, R., Moresoli, C., Yu, A., Yuan, Z., and Xu, C. (2020). Poly (lactic acid)/acetylated starch blends: effect of starch acetylation on the material properties. *Carbohydr. Polym.* 229:115453. doi: 10.1016/j.carbpol.2019.115453
- Peerajit, P., Chiewchan, N., and Devahastin, S. (2022). Effects of pretreatment methods on health-related functional properties of high dietary fiber powder from lime residues. *Food Chem.* 132, 1891–1898. doi: 10.1016/j.foodchem.2011.12.022
- Qin, X., Yang, C., Si, J., Chen, Y., Xie, J., Tang, J., et al. (2023). Fortified yogurt with high-quality dietary fiber prepared from the by-products of grapefruit by superfine grinding combined with fermentation treatment. *LWT-Food Sci. Technol.* 188:115396. doi: 10.1016/j.lwt.2023.115396
- Rashwan, A. K., Karim, N., Shishir, M. R. I., Bao, T., Lu, Y., and Chen, W. (2020). Jujube fruit: a potential nutritious fruit for the development of functional food products. *J Func. Foods.* 75:104205. doi: 10.1016/j.jff.2020.104205
- Sang, J. Q., Li, L., Wen, J., Liu, H. C., Wu, J. J., Yu, Y. S., et al. (2022). Chemical composition, structural and functional properties of insoluble dietary fiber obtained from the Shatian pomelo peel sponge layer using different modification methods. *LWT-Food Sci. Technol.* 165:113737. doi: 10.1016/j.lwt.2022.113737
- Shaikh, M., Haider, S., Ali, T. M., and Hasnain, A. (2019). Physical, thermal, mechanical and barrier properties of pearl millet starch films as affected by levels of acetylation and hydroxypropylation. *Int. J. Biol. Macromol.* 124, 209–219. doi: 10.1016/j.ijbiomac.2018.11.135
- Si, J. Y., Yang, C. R., Chen, Y., Xie, J. H., Tian, S. L., Cheng, Y. A., et al. (2023). Structural properties and adsorption capacities of Mesona chinensis Benth residues dietary fiber prepared by cellulase treatment assisted by aspergillus Niger or Trichoderma reesei. *Food Chem.* 407:135149. doi: 10.1016/j.foodchem.2022.135149
- Siddiqui, H., Sultan, Z., Yousuf, O., Malik, M., and Younis, K. (2023). A review of the health benefits, functional properties, and ultrasound-assisted dietary fiber extraction. *Bioact. Carbohydr. Diet. Fibre* 30:100356. doi: 10.1016/j.bcdf.2023.100356
- Tapia-Hernández, J. A., Del-Toro-Sánchez, C. L., Cinco-Moroyoqui, F. J., Juárez-Onofre, J. E., Ruiz-Cruz, S., Carvajal-Millan, E., et al. (2019a). Prolamins from cereal by-products: classification, extraction, characterization and its applications in micro- and nanofabrication. *Trends Food Sci. Technol.* 90, 111–132. doi: 10.1016/j.tifs.2019.06.005
- Tapia-Hernández, J. A., Del-Toro-Sánchez, C. L., Cinco-Moroyoqui, F. J., Ruiz-Cruz, S., Juárez, J., Castro-Enriquez, D. D., et al. (2019b). Gallic acid-loaded Zein nanoparticles by Electro spraying process. *J. Food Sci.* 84, 818–831. doi: 10.1111/1750-3841.14486
- Torbica, A., Radosavljević, M., Belović, M., Djukić, N., and Marković, S. (2022). Overview of nature, frequency and technological role of dietary fibre from cereals and pseudocereals from grain to bread. *Carbohydr. Polym.* 290:119470. doi: 10.1016/j.carbpol.2022.119470
- Xia, X., Li, F., Ran, H., Zhao, J., Lei, X., Lei, L., et al. (2023). Effect of jujube kernel powder addition on moisture absorption performance, color stability, texture properties and agglomeration characteristics of jujube powder. *LWT-Food Sci. Technol.* 174:114452. doi: 10.1016/j.lwt.2023.114452
- Zadeike, D., Vaitkeviciene, R., Degutyte, R., Bendoraitiene, J., Rukuiziene, Z., Cernauskas, D., et al. (2021). A comparative study on the structural and functional properties of water-soluble and alkali-soluble dietary fibers from rice bran after hot-water, ultrasound, hydrolysis by cellulase, and combined pre-treatments. *Int. J. Food Sci. Technol.* 57, 1137–1149. doi: 10.1111/ijfs.15480
- Zhang, S., Dong, Z., Shi, J., Yang, C., Fang, Y., Chen, G., et al. (2022). Enzymatic hydrolysis of corn Stover lignin by laccase, lignin peroxidase, and manganese peroxidase. *Bioresour. Technol.* 361:127699. doi: 10.1016/j.biortech.2022.127699
- Zheng, Y. J., and Li, Y. (2018). Physicochemical and functional properties of coconut (Cocos nucifera L.) cake dietary fibres: effects of cellulase hydrolysis, acid treatment and particle size distribution. *Food Chem.* 257, 135–142. doi: 10.1016/j.foodchem.2018.03.012
- Zheng, Y. J., Li, J. R., Wang, X. Y., Guo, M., Cheng, C. X., and Zhang, Y. (2023). Effects of three biological combined with chemical methods on the microstructure, physicochemical properties and antioxidant activity of millet bran dietary fibre. *Food Chem.* 411:135503. doi: 10.1016/j.foodchem.2023.135503
- Zheng, Y., Xu, B., Shi, P., Tian, H., Li, Y., Wang, X., et al. (2022). The influences of acetylation, hydroxypropylation, enzymatic hydrolysis and crosslinking on improved adsorption capacities and in vitro hypoglycemic properties of millet bran dietary fibre. *Food Chem.* 368:130883. doi: 10.1016/j.foodchem.2021.130883
- Zhu, L., Yu, B., Chen, H., Yu, J., Yan, H., Luo, Y., et al. (2022). Comparisons of the micronization, steam explosion, and gamma irradiation treatment on chemical composition, structure, physicochemical properties, and in vitro digestibility of dietary fiber from soybean hulls. *Food Chem.* 366:130618. doi: 10.1016/j.foodchem.2021.130618
- Zohaib, H., Muhammad, I., Haseeb, A. M., and Kamran, K. M. (2021). Ultrasound-assisted modification of insoluble dietary Fiber from chia (*Salvia hispanica* L.). *Seeds. J Food Quality.* 2021, 1–10. doi: 10.1155/2021/5035299